Revista de Metalurgia
July-September 2023, 59 (3), e245
ISSN-L: 0034-8570
https://doi.org/10.3989/revmetalm.245

Optimization on the electrical discharge machining (EDM) process parameters of aged AA7075/TiC metal matrix composites

Prabu Rajendran[a,*], Velmurugan Duraisamy[b], Ashok Raj Rajendran[c], Raja Velur Loganathan[d]

[a] Assistant Professor, Department of Mechanical Engineering, Mahendra Engineering College, (Autonomous), Namakkal, India

[b] Associate Professor Department of Mechanical Engineering, Muthayammal Engineering College, (Autonomous), Namakkal, India

[c] Associate professor, Department of Mechanical Engineering, J.J. College of Engineering & Technology, Trichy, India

[d] Professor, Department of Mechanical Engineering, Loyola Institute of Technology, Chennai, India

(*Corresponding author: enggprabuams@gmail.com)

Submitted: 12 January 2023; Accepted: 21 November 2023; Available On-line: 3 January 2024

ABSTRACT: The need to optimize the process parameters in Electrical Discharge Machining (EDM) for aged AA7075 Metal Matrix Composites (AAMMCs) is evident as it impacts various aspects such as mechanical properties, tool wear, surface finish, integrity, precision, accuracy, process stability, process consistency, and cost-effectiveness. In this study, aluminium alloy AA7075 was chosen as the matrix material because of the need to enhance its mechanical properties. Titanium Carbide (TiC) was chosen as the reinforcing material owing to its superior mechanical properties. Therefore, TiC holds the capability to improve the mechanical attributes of AA7075. The selection of the stir cast method for the manufacturing of AA7075/TiC (0, 4, 8, 12, and 16 wt.%) was based on its ease of fabrication, ability to achieve a uniform distribution of reinforcements, reduced susceptibility to oxidation and porosity, and improved control over the microstructure. This AA7075/12wt.%TiC MMC underwent an aging process at 520 °C for 180 min and was subsequently cooled within the furnace environment. The density of the aged and non-aged AA7075/TiC-based composites was determined through a density test using the Archimedes' principle. Microhardness testing was conducted on the non-aged and aged AA7075-based MMCs employing a Vickers microhardness tester. Tensile strength and compressive strength of the aged and non-aged AA7075-based MMCs were determined by the usage of a universal testing machine (UTM) and a compression testing machine (CTM). The optimal combination of the manufactured AA7075/TiC MMCs was determined based on their mechanical properties. The most effective combination was identified as AA7075/12wt.%TiC MMC due to its superior values in hardness, tensile strength, compressive strength, and density compared to other combinations. The aging process aimed to enhance the mechanical properties without the need for additional reinforcements. EDAX and X-ray Diffraction Analysis (XRD) tests were employed to determine the weight percentage of the matrix and reinforcements and to identify the formation of precipitates in the AA7075/12wt.%TiC composites. The SEM equipment was utilized to verify the uniform distribution of titanium carbide in the matrix material AA7075. Optimization of EDM process parameters for aged AA7075/12wt.%TiC composite was carried out using Taguchi design-based Grey Relational Analysis (GRA). The selected input parameters for the optimization included the chromium concentration ($g \cdot l^{-1}$), current (amps) and pulse-on time (µs). The response parameters chosen for optimization were surface roughness (SR) and tool wear rate (TWR). The sequence of influencing EDM input parameters is chromium concentration, pulse on time and current. The optimized EDM process parameters were 8 $g \cdot l^{-1}$ chromium concentration, 5 amps current and 240 µs pulse on time and the corresponding response were 0.198 TWR and 1.56 SR.

KEYWORDS: AA7075; Density; Electrical discharge machining; Microhardness; Stir casting; Surface roughness; TiC; Tool wear rate

Citation/Citar como: Prabu Rajendran; Velmurugan, D.; Ashok Raj, R.; Raja, V.L. (2023). "Optimization on the electrical discharge machining (EDM) process parameters of aged AA7075/TiC metal matrix composites". *Rev. Metal.* 59(3): e245. https://doi.org/10.3989/revmetalm.245

RESUMEN: *Optimización de los parámetros del proceso de mecanizado por electroerosión (EDM) de materiales compuestos de matriz metálica AA7075/TiC envejecidos.* La necesidad de optimizar los parámetros de proceso en el mecanizado por descarga eléctrica (EDM) para materiales compuestos de matriz metálica AA7075 envejecidos (MCMM) es evidente ya que afecta a varios aspectos como las propiedades mecánicas, el desgaste de la herramienta, el acabado superficial, la integridad, la precisión, la exactitud, la estabilidad del proceso, la consistencia del proceso y la rentabilidad. En este estudio, se eligió la aleación de aluminio AA7075 como material matriz debido a la necesidad de mejorar sus propiedades mecánicas. El carburo de titanio (TiC) se eligió como material de refuerzo debido a sus propiedades mecánicas superiores. Por lo tanto, el TiC tiene la capacidad de mejorar los atributos mecánicos del AA7075. La selección del método de colada por agitación para la fabricación del AA7075/TiC (0, 4, 8, 12 y 16% en peso) se basó en su facilidad de fabricación, su capacidad para lograr una distribución uniforme de los refuerzos, la menor susceptibilidad a la oxidación y la porosidad, y el mejor control sobre la microestructura. Este MCMM AA7075/12%TiC se sometió a un proceso de envejecimiento a 520 °C durante 180 min y posteriormente se enfrió en el entorno del horno. La densidad de los materiales compuestos AA7075/TiC envejecidos y no envejecidos se determinó mediante un ensayo de densidad utilizando el principio de Arquímedes. Se realizaron ensayos de microdureza en los MCMMs sobre la aleación AA7075 envejecida y no envejecida empleando un medidor de microdureza Vickers. Se determinó la resistencia a la tracción y a la compresión de los MCMMs tanto envejecidos como no envejecidos mediante el uso de una máquina universal de ensayos mecánicos y una máquina de ensayos de compresión. Se determinó la combinación óptima de los MCMMs fabricados (AA7075/TiC) en función de sus propiedades mecánicas. Basados en estos resultados, el MCMM más prometedor fue la combinación AA7075/12%TiC debido a sus valores superiores en dureza, resistencia a la tracción, resistencia a la compresión y densidad en comparación con otras combinaciones. El proceso de envejecimiento tenía como objetivo mejorar las propiedades mecánicas sin necesidad de refuerzos adicionales. Se emplearon microanálisis EDAX y análisis de Difracción de Rayos X (DRX) para determinar el porcentaje en peso de la matriz y los refuerzos e identificar la formación de precipitados en el material compuesto AA7075/12%TiC. Se utilizó microscopía electrónica de barrido (MEB) para verificar la distribución uniforme del carburo de titanio en la matriz AA7075. La optimización de los parámetros del proceso de electroerosión para el MCMM AA7075/12%TiC envejecido se llevó a cabo utilizando el análisis relacional gris (GRA) basado en el diseño de Taguchi. Entre los parámetros de entrada seleccionados para la optimización, se incluyeron la concentración de cromo ($g \cdot l^{-1}$), la corriente (amperios) y el tiempo de pulsación (µs). Los parámetros de respuesta elegidos para la optimización fueron la rugosidad superficial (SR) y la tasa de desgaste de la herramienta (TWR). La secuencia de influencia de los parámetros de entrada de EDM es la concentración de cromo, el tiempo de pulso y la corriente. Los parámetros del proceso de electroerosión optimizados fueron 8 $g \cdot l^{-1}$ de concentración de cromo, 5 amperios de corriente y 240 µs de tiempo de pulso, y las respuestas correspondientes fueron 0,198 TWR y 1,56 SR.

PALABRAS CLAVE: AA7075; Densidad; Fundición por agitación; Mecanizado por electroerosión (EDM); Microdureza; Rugosidad superficial; Tasa de desgaste de la herramienta; TiC

ORCID ID: Prabu Rajendran (https://orcid.org/0000-0001-5057-8765); Velmurugan Duraisamy (https://orcid.org/0000-0002-5392-3461); Ashok Raj Rajendran (https://orcid.org/0000-0003-3726-4635); Raja Velur Loganathan (https://orcid.org/0000-0002-0327-2816)

1. INTRODUCTION

The focal point of this manuscript is to outperform market competition, adhere to strict emission regulations for environmental preservation, tackle the energy-deficient global situation, and reduce pollution to safeguard the Earth. Utilizing modern materials for weight reduction stands out as a highly promising strategy, delivering fuel efficiency without compromising vehicle performance. The introduction of lightweight composite materials, possessing comparable strength and more appealing features than traditional materials, has captured the attention of both enterprises and researchers for potential applications across various sectors. These materials demonstrate favorable characteristics, such as outstanding corrosion resistance, an optimal strength-to-weight ratio, high stiffness, adaptability, and various opportunities for functional integration (Burande *et al.*, 2021). Moreover, conventional alloys are being substituted with novel composite materials due to the shortcomings of conventional alloys in terms of structural, tribological, and corrosion resistance properties (Bandil *et al.*, 2019). The utilization of aluminum alloys for structural purposes has experienced substantial growth in recent years, driven by their favorable properties. These include a ease of fabrication, high strength-to-weight ratio, excellent workability, significant ductility, efficient thermal con-

ductivity, notable corrosion resistance, and an aesthetically pleasing appearance in their untreated state. Consequently, the construction industry currently accounts for 25% of global aluminum production (Foster *et al.*, 2015). The density of materials exerts diverse effects, influencing factors like weight reduction, strength-to-weight ratio, corrosion resistance, ease of production, and suitability across various industries and applications. The microhardness of materials plays a major role in shaping their mechanical and functional characteristics. It is a gauge of the material's ability to resist indentation or penetration at a microscopic level. The ability of materials to carry and distribute loads is directly linked to their tensile strength. Materials with elevated tensile strength can endure more substantial loads, rendering them suitable for applications involving load-bearing, such as structural components in aircraft or automotive engineering. The machinability and formability of materials can be influenced by their compressive strength. A material with elevated compressive strength might pose challenges in machining and molding processes, thereby affecting production operations. The significance of impact strength is undeniable in numerous industries and applications where materials encounter sudden dynamic loads. It influences the selection of materials, design parameters, safety considerations, and the overall performance and durability of products and structures. Materials exhibiting robust resistance to creep are essential for aviation engines and components. This is due to the fact that these components routinely operate under extreme temperatures for prolonged durations. The utilization of creep-resistant materials significantly enhances the structural integrity and reliability of critical engine components. Fatigue is the progressive and localized structural degradation that occurs as a material experiences repeated cycles of loading and unloading.

Recognizing and considering the fatigue characteristics of materials is essential for constructing durable and reliable components across various industries. Ductility is the term used to describe a material's ability to experience substantial plastic deformation before reaching rupture or fracture. Malleability, on the other hand, refers to a material's ability to endure deformation under compressive stress, enabling it to be shaped or hammered into thin sheets without breaking. Diverse fabrication methods are employed to form and shape materials into finished products or components. The choice of manufacturing processes is influenced by the properties of the material, the complexity of the design, and the intended application, and the different fabrication methods are casting, machining, forging, stamping, extrusion, injection molding, additive manufacturing, welding, brazing, and powder metallurgy. The 7xxx series of aluminum alloy has been employed in structural applications for the past several years. The aluminum alloys classified as "7XXX," commonly referred to as AA7XXX, are predominantly composed of aluminum-zinc-magnesium (Al-Zn-Mg) alloys. Renowned for their elevated strength-to-weight ratio, excellent corrosion resistance, and formability, these alloys are widely recognized in various applications. They possess good strength, high corrosion resistance, excellent formability, weldability, heat-treatability, moderate to high fatigue strength, and moderate electrical conductivity. AA7075 is widely employed for manufacturing aerospace components, military parts, high-performance sports equipment, automotive components, marine structures, rock climbing gear, high-pressure vessels, and machinery parts. While aluminum alloy AA7075 is noted for its better strength-to-weight ratio and great performance in a variety of applications, it also has limits and concerns such as susceptibility to stress corrosion cracking, limited weldability, high cost, lower formability, unsuitability for elevated temperature applications, brittleness in the overaged condition, and limited availability in some forms. In recent years, the properties of AA7075 do not meet the requirements of various industries used for manufacturing automobile components, marine (Rometsch *et al.*, 2014; Zhou *et al.*, 2021). Novel composites are produced with high strength-to-weight ratio, high corrosion resistance, ductility, toughness, and high fatigue resistance to replace AA7075 in various applications (Khan *et al.*, 2022). The density of AA7075/B4C MMCs was reduced while adding boron carbide by the powder metallurgy technique. The hardness of AA7075/B4C MMC increased after subjecting it to heat treatment. The hardness of the 20% B4C fortified AA7075 sample before heat treatment was 95.34, and it increased to 102 after heat treatment (Seyit *et al.*, 2023). The CNMG-EM insert of grade 6615 demonstrates a tool life of 8.81 minutes during the turning of AA7075/15 wt% SiC (10-20 m). This operation occurs at a feed of 0.15 mm, cutting speed of 90 $m \cdot min^{-1}$, nose radius of 0.4 mm and a depth of cut of 0.41 mm. Across all cutting parameters, the tool life diminishes with increasing particle volume fraction and cutting speed. Research indicates that the DOC exerts the most substantial physical and statistical impact on tool life, with the weight percentage and size of silicon carbide particles following in significance (Kumar Bhushan *et al.*, 2023). In contrast to conventional metals, nanocomposites exhibit reduced wear rates.

A reduction in wear rate and friction coefficient is observed with an escalation in SiC weight percentage, especially at elevated sliding speeds and SiC weight fractions. The presence of SiC and other phases in the composites is verified through FESEM analysis. Significantly, the composite with 4 wt% SiC surpasses the Al 7075 matrix metal in terms of friction coefficient, weight loss and wear rate (Phaneendra *et al.*, 2023). The hardness, ultimate tensile strength (UTS) and yield strength (YS) exhibit an increase with higher graphite inclusion and longer milling duration. However, elongation to fracture decreases under these conditions. Simultaneously, the recrystallized grain size diminishes with an increase in both milling duration and graphite concentration. Moreover, in accordance with the Hall-Petch relationship, changes in yield strength are associated with variations in grain size. The observed hardening of the AA7075-Gr composites is attributed to factors such as grain refinement, formation of Mg_2Zn_2, Al_4C_3, and Al_2O_3, as well as the creation of a random texture, albeit to a lesser extent (Gutiérrez *et al.*, 2023). To achieve the required strength enhancement in Fe1.2NiCrCoAlTi0.8 particles (HEAp) reinforced AA7075 alloy, the optimum input combinations include a pressure of 75.2 MPa, 11.7% HEA, and a sintering temperature of 447.7 °C (Ogunbiyi *et al.*, 2023). To enhance wear resistance and contact performance, materials like B_4C and MoS_2 are incorporated into AA7075 composites. Additionally, the introduction of fly ash and Al_2O_3 particles contributes to improved micro-hardness and overall mechanical properties (Sharma *et al.*, 2023). The increase in the wt.% of reinforcing particles leads to enhanced wear resistance. Additionally, the continuous reinforcement of Al_2O_3 and SiC particles contributes to improved mechanical and wear characteristics (Rao *et al.*, 2023). In comparison to both acidic and basic solutions, the overall corrosion resistance is considerably lower in aqueous solutions for all composites. However, under both acidic and basic conditions, the composite containing 4% TiB_2 displays the high corrosion rate (Manojkumar *et al.*, 2023). The behaviour of four distinct textured drills is evaluated in comparison to a non-textured drill. These textured drills include, a groove on the flute , perpendicular grooves on the margin a dimple on the flute, and parallel grooves on the margin. Among these, the dimple-textured drill demonstrates superior behaviour due to the enhanced micro-PL effect provided by micro-dimples in the flute zone (Selvakumar *et al.*, 2023). The successful application of the Taguchi technique leads to the identification of optimal values for input variables, maximizing impact strength, hardness and tensile strength. The experiment reveals that the most favorable parameters are a stirring speed of 600 rpm, a temperature of 600 °C, and a TiO_2 content of 9 wt%. The model's R square value of 99.5% indicates a complete fit. The highest Brinell hardness is attained under the following conditions: (i) temperature of 660 °C, (ii) stirring speed of 600 rpm, and (iii) a reinforcement percentage of 6 wt% (Nithya *et al.*, 2023). The dynamic responses of AA7075 and TiC/AA7075 specimens, fabricated using Arc-DED, are examined in as-built and heat-treated conditions. This investigation is conducted through Split-Hopkinson pressure bar tests at room temperature, covering strain rates from 2000 to 5000 s^{-1}. The results suggest that the inclusion of TiC nanoparticles enhances the dynamic characteristics of AA, particularly after heating process. The observed improvement is characterized to the refined grain and the resulting betetr phase in the material (Rui *et al.*, 2023). The aluminum alloys based composites are manufactured by utilizing various techniques such as powder metallurgy, stir casting, centrifugal casting, and additive manufacturing methods (Pulkit *et al.*, 2019; Verma *et al.*, 2021). The stir casting technique is a very cheap and simple method for manufacturing aluminum alloys based composites (Pradhan *et al.*, 2016; Sharma *et al.*, 2020). Different hard reinforcements such as Silicon Carbide (SiC), Boron Carbide (B_4C), Aluminum dioxide (Al_2O_3), Titanium Boride (TiB_2), Titanium Carbide (TiC), Silicon Nitride (Si_3N_4) Titanium dioxide (TiO_2) and Tungsten Carbide (WC) are widely employed for reinforcing aluminum alloys (Neuman *et al.*, 2017; Meignanamoorthy *et al.*, 2020; Bharat and Bose, 2022a). The aging process is needed for enhancing the hardness of the aluminum alloys for using in various applications. Besides, the aging of aluminum alloys based composites causes an increase in the usage of aluminum alloy-based composites in different applications (Viswanatha *et al.*, 2021a). The increased hardness may be attributed to significant morphological changes occurring during mechanical deformation, including microstructural refinement, densification, and improved homogeneity. For the AA 7075 aluminum alloy, it is recommended to undergo hot deformation at 400 °C and subsequent aging at the same temperature for altering both dimensional and mechanical characteristics (Vikas *et al.*, 2021). The findings indicate that the natural aging process can significantly improves the strength of AA7075 due to the creation of clusters in the AA matrix. This, in turn, expedites the precipitation of the 'phase during subsequent artificial aging treatment (Tai *et al.*, 2022). Enhancements in microhardness and wear resistance were achieved by elevating the heating temperature and prolonging the heating time. In comparison to alternative cooling conditions, furnace cooling yielded superior microhardness and wear resistance. The optimized parameters for the age-hardening process were determined to be a hardening temperature of 400 °C, a hardening duration of 270 min, and furnace cooling as the preferred cooling environment. These parameters led to improved mechanical and tribological characteristics through increased precipitate formation and density augmentation (Ashok Raj *et al.*, 2023). The optimization of EDM process parameters on various composites is done to improve the machining characteristics. The optimization is done by using various techniques such as Taguchi technique, TOPSIS, GRA, and various algorithms (Balaji *et al.*, 2023).

Elevating the machining current in AA7075-SiC Composites results in an increased TWR. Therefore, an optimal current of 12 amps is recommended for machining these composites. Through PCA Taguchi analysis, the identified optimal parameters include a current of 12 amps, pulse on time of 15 s, pulse off time of 1 s, and voltage of 35V. Experimental results indicate that while increasing the current enhances the

MRR, it also leads to higher Tool Wear Rate (TWR) and reduced surface smoothness (Bharat and Bose, 2022b). The research demonstrated that the TWR rises from 6 amps to 15 amps and remains relatively constant beyond this current range. Sensitivity Analysis highlights that, among the parameters studied, current has the most significant influence on the outcomes of the trials (Prasanna *et al.*, 2017). Utilizing stir casting, AA7075-SiC composites were effectively produced. The parameters of EDM, including current, pulse on time, and voltage, were fine-tuned to enhance surface roughness and achieve the maximum MRR. The optimized parameters for improved surface finish were identified as A3B2C1 and A2B1C2 for achieving the highest MRR. The outcomes from Taguchi's analysis align entirely with the results obtained from ANOVA (Sakthivelu *et al.*, 2020). TWR increased with increasing peak current and pulse length, however there was no significant fluctuation with varying gap voltages. SR was discovered to have a substantial rising tendency with increasing current and pulse length. However, when the gap voltage increased, SR showed a changing tendency (Bharat and Bose, 2021; Gupta *et al.*, 2022). Based on the experimental results, it is indicated that the key factors impacting the material removal rate are the pulse ON time and pulse current. As for surface roughness and the electrode wear ratio, the most influential parameters are identified as pulse ON time and electrode material (Alagarsamy and Ravichandran, 2021; Bharat and Bose, 2023). The addition of titanium carbide improves the mechanical properties of the AA2024 based composites. The higher microhardness is obtained in the AA2024/TiC composites (Sairam Varma *et al.*, 2018). The inclusion of titanium carbide improves the wear resistance of the AA356/TiC composites. The higher wear resistance is obtained in AA356/TiC composite (Kakaravada *et al.*, 2020). The addition of TiC into AA6061 matrix material improves the corrosion resistance of the AA6061/TiC composites. The higher corrosion resistance is obtained in AA6061/TiC composites (Chi *et al.*, 2021). The aging of AA7075/WC composites enhanced the hardness, compressive strength and impact strength of AA7075/WC composites (Rajaram *et al.*, 2022). The optimization on EDM process parameters of AA7075/SiC is done by using L16 orthogonal array. The optimized influenced sequence of EDM process parameters of AA7075/TiO_2 composites are pulse on, pulse off and current (Balaji *et al.*, 2023). Conducted experiments on AISI D2 steel involved the incorporation of additives into the dielectric to analyze and enhance the surface properties of the steel, leading to improved surface finish during cutting (Kumar, 2014). According to the experimental findings and GRA, the best process parameters for achieving the maximum grey relational grade (GRG) are a a spindle speed of 3000 rpm, Carbide drill material, feed rate (F) of 50 $m \cdot s^{-1}$, and 6% reinforcement (Jebarose *et al.*, 2023).

The hybrid Taguchi-GRA-PCA strategy for optimizing wear behavior process factors has been painstakingly created to overcome the constraints of single-objective methodologies in issues with numerous performance characteristics (Prianza *et al.*, 2020; Bharat and Bose, 2023). The use of Taguchi and GRA techniques considerably proves that the effect of speed as beahviour element is greater than load, which is a stronger factor than wt.% of reinforcements (Ikubanni *et al.*, 2021)

Based on the literature review, it is concluded that there has been no research conducted on the fabrication and aging of AA7075/TiC MMCs using stir casting equipment and a furnace. Additionally, there is a lack of research on the optimization of the EDM process parameters for aged AA7075/TiC composites. Previous studies have researched only the fabrication of AA7075/TiC MMCs and also the optimization of EDM process parameters of AA7075 MMCs without applying and aging treatment. Besides, no previous research has been done by taking into account the wt.% of chromium additive as one of the input parameters during the optimization of EDM process parameters on AA7075/TiC MMCs. In this research, the optimization of EDM process parameters for aged AA7075/TiC composite is performed using grey relational analysis (GRA), with the selection of current, chromium concentrations and pulse-on time as input parameters, and tool wear rate (TWR) and surface roughness (SR) as response parameters. The novelty of this research lies in optimizing EDM process parameters for aged AA7075/TiC by incorporating the chromium concentrations as one of the EDM input parameters. Previous studies have utilized additives with dielectric fluid, but none have investigated the use of chromium additives as an input parameter in EDM. The optimized weight percentage of chromium as an additive with the dielectric fluid is expected to influence the TWR and SR of AA7075/TiC MMCs.

2. MATERIALS AND METHODS

2.1. Materials

AA7075 found widespread application in aerospace where the demand for better strength and low weight was critical. Additionally, it was employed in the fabrication of structural components for the automotive industry and the construction of high-performance bicycle frames. AA7075, a representative Al-Zn- Cu Mg alloy, stood as the most extensively researched series among aluminum alloys. Within the 7xxx series, it held pre-eminence due to its exceptional combination of properties, encompassing high strength, heightened toughness, excellent electrical and thermal conductivity, notable wear and abrasion resistance, resilience to damage at elevated temperatures, commendable creep resistance, fatigue strength and the higher failure elongation. This versatility rendered it the preferred choice across diverse sectors, including submarines, aerospace, ships, prosthetic devices, rail vehicles, pressure vessels, trucks, machinery, and aircraft components such as lower drag brace ventral fins, landing gears and helicopter blades. Its utility further extended to electronics, military applications, and the automotive industry, where it found application in brake calipers, pistons, wheels and rocker arms. The AA7075 aluminum alloy was renowned for its impressive strength-to-weight ratio and was part of the 7000 series of aluminum alloys, recognized for their exceptional strength. The designation "AA" in AA7075 represented the Aluminum Association, the entity responsible for categorizing aluminum alloys. AA7075 was distinguished by its formidable strength, comparable to that of many steels, and was often employed in applications requiring robustness. Additionally, being heat-treatable, AA7075 allowed for the enhancement of its mechanical properties through heat treatment, facilitating the customization of the alloy's characteristics for specific purposes. While aluminum, known for its robust corrosion resistance, generally exhibited this property well, AA7075, unlike some other aluminum alloys, particularly those in the 6000 series, was not as corrosion resistant; furthermore, AA7075 was commonly considered to have poor weldability, requiring careful welding procedures to minimize cracking, and post-welding heat treatment might be necessary. AA7075 demonstrated moderate machinability, allowing for machining through conventional processes. However, its considerable strength might present challenges related to tool wear during machining. AA7075 exhibited robust fatigue resistance, rendering it suitable for applications with cyclic stress. Despite its notable strength, AA7075 might possess less resilience compared to certain other aluminum alloys. Toughness, a measure of a material's ability to withstand energy and subjects to plastic deformation before fracturing, was a key aspect to consider. The moderate properties of AA7075 were not enough to fulfil the requirements of the fastest-growing industries such as military, automobile and marine. Hence, the aluminum alloy needed enhancement of mechanical properties (Huda A and Vignesh Kumar V). So, the aluminum alloy 7075 was nominated as the matrix material in this investigation. The titanium carbide was nominated as reinforcements because of its excellent mechanical properties. Titanium carbide (TiC), a refractory ceramic known for its elevated hardness, exceptional wear resistance, and high thermal conductivity, was well-suited for applications requiring efficient heat transmission. Its sought-after properties, including wear resistance, made it ideal for cutting tools, wear-resistant coatings, and scenarios demanding resistance to abrasion. Moreover, titanium carbide typically displayed corrosion resistance, rendering it appealing for use in corrosive environments, further complemented by its inherent hardness. The AA7075 was acquired from Trichy metals, Trichy, Tamil Nadu, India, and it was acquired in cylindrical rod form. The titanium carbide reinforcement was acquired from Sigma Ulrich. The TiC was acquired in the form of powder with a particle size of 10 µm. The particle size of titanium carbide was measured by employing Particle Size Analyzer (PSA). The SEM image of reinforcement TiC is displayed in Fig. 1. The shape of the titanium carbide was elliptical, and it was easily bonded with the matrix material, and the load-carrying capacity was also high. Elliptical shapes, in contrast to spherical particles, could provide enhanced reinforcement along specific orientations. The improved fracture arrest capabilities

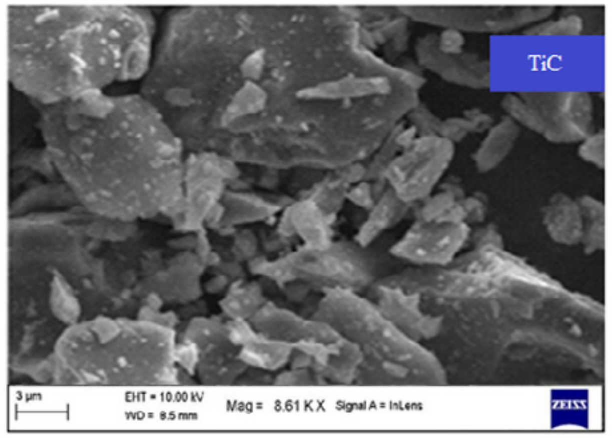

Figure 1. SEM image of TiC.

Table 1. Chemical composition of Al7075

Elements	Ti	Mg	Fe	Si	Cr	Zn	Mn	Cu	Al
Wt.%	0.08	2.5	0.23	0.09	0.21	5.99	0.05	1.6	Bal.

Table 2. Properties of matrix and reinforcements

Property	TiC	Al7075
Tensile Strength	338	256 MPa
Melting Point	3170 °C	800 °C
Poisson ratio	0.27	0.3
Density	4.94 g/cm³	2.81 g/cm³
Modulus of Elasticity	412	190 GPa
Purity	99	99.5
Particle size	10 µm	-

of elliptical forms, compared to spherical particles, contributed to increased toughness. The crack propagation was easily prevented by this elliptical shape of TiC. The elements presented in the AA7075 are displayed in Table 1, (HassabAlla *et al.*, 2022). The details of AA7075 and TiC are displayed in Table 2.

2.2. Fabrication and ageing of composites

The AA7075/xTiC (x=0, 4, 8, 12, and 16 wt.%) MMCs were manufactured by utilizing the stir casting setup. The flow chart of the stir casting process of AA7075/TiC MMCs was displayed in Fig. 2. The stir casting setup was displayed in Fig. 3. The acquired AA7075 was sized into a small cylindrical rod by a hacksaw. The reinforcement TiC was preheated at 250 °C for a duration of 30 min. The small-sized matrix AA7075 was placed into the crucible furnace of the stir casting setup. The furnace was heated to 800 °C, the melting temperature of the AA7075 matrix material (Agrawal, *et al.*, 2023). The preheated titanium carbide was fed into the crucible furnace of the stir casting setup to mix with the melted AA7075 matrix material. 2 wt.% of magnesium was included in the crucible furnace to improve the bonding between the AA7075 and TiC (Sethi *et al.*, 2020). The mechanical stirrer was utilized to mix the melted matrix AA7075 material and TiC reinforcement. The stirrer was rotated at a speed of 300 rpm for a rotating duration of 10 min. The mixed AA7075 and TiC were poured into the die to solidify the mixed AA7075/TiC composite material. The square-sized die with dimensions of 152x152x22 mm³ was used

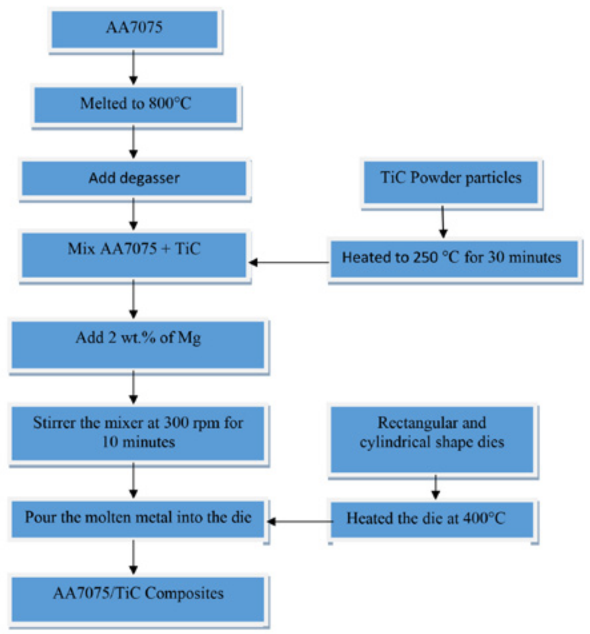

Figure 2. Flow chart for stir casting process of AA7075/TiC composites.

Figure 3. Stir casting setup.

for stir casting of AA7075/TiC MMCs, and also, a cylindrical-shaped die with a diameter of 32 and a length of 120 mm was used. The casted sample sizes were 100x100x10 mm and 100 mm length x 20 mm diameter. The same procedure was repeated for manufacturing the AA7075/xTiC (x=0, 4, 8, 12, and 16 wt.%) MMCs. The casted AA7075/TiC composites were further aged at 520 °C for a duration of 3 h in the electrical muffle furnace, and the heated AA7075/TiC composite was quenched in water. The quenched AA7075/TiC composites were further heat-treated at 250 °C for a duration of 4 h, and they were cooled in the muffle furnace itself. The aging procedure was followed for aging the AA7075/xTiC (x=0, 4, 8, 12, and 16 wt.%) MMCs.

2.3. Testing of composites

The micro hardness, tensile, compressive, and density tests were conducted on aged AA7075/xTiC (x=0, 4, 8, 12, and 16 wt.%) MMCs to measure the Vickers microhardness, the compressive strength, tensile strength and density. The aged AA7075-based composites were cut into the required ASTM standard shape by utilizing wire cut EDM. The Archimedes principle was utilized to find the density of the aged AA7075/TiC composites. The microhardness of aged AA7075/TiC composites was determined by conducting a hardness test as per ASTM E384 with the help of a Vickers hardness tester (M V - 5, R 1 – 2970 HV). The Vickers hardness test was conducted at the loading condition of 300 g for a loading duration of 10 s. Three trials were done, and the average value had been taken. A composite material's performance under axial stretching force was assessed through a tensile test, conducted employing a 10 kN Instron computerized universal testing machine (UTM). The test samples were manufactured in adherence to the ASTM E08 standard. The tensile fractured surface was analyzed by utilizing a scanning electron microscope (SEM) to determine the fracture mechanism. The compression test utilized a computerized UTM (UNIVERSAL 2001 - UTE 40) with a 40 KN load capacity. Test samples were manufactured following the ASTM E9 standard. The compressive strength was measured at a crosshead speed of 2 mm·min^{-1}. The best combination of aged AA7075/TiC composites was determined based on its density, microhardness, tensile strength, and compressive strength. The X-ray diffraction analysis and EDAX microanalysis were done on the best combination of AA7075/TiC composites. The microstructure of the best combination of AA7075/TiC composites was characterized using scanning electron microscopy. This aged AA7075/TiC composite was polished by employing 600, 800, 1000, and 1200 grit sheets. The surface roughness of polished aged AA7075/TiC composite was about 1 µm. To reveal the microstructure AA7075/TiC composite was etched using Keller's reagent. The constituents of Keller's reagent were 2.5 ml HNO_3, 1.5 ml HCl, 1 ml HF and 95 ml Distilled Water (Kumar *et al.*, 2023). The enhancement of micro hardness causes it to be very hard to machine, and hence the determination of the optimized parameters of machining is needed (Bharat and Bose, 2023). The EDM parameters were optimized for best aged AA7075/TiC composite. The EDM model used is SPARKONIX India Pvt. The dielectric fluid was mixed with chromium for obtaining a better machining surface. The chromium concentration (0, 4, 8 g/litre), pulse on time (120, 240, and 360 µs), and current (5, 10, and 15 amps) were chosen as input parameters (Sivasamy *et al.*, 2021).

The pulse-on time, also known as the "on-time" or "pulse duration", denoted the duration of an electrical discharge or spark between the electrode and the work piece. This interval encompassed the generation of a high-frequency electrical discharge that produced intense heat concentrated at a specific location on the work piece. As a result of this concentrated heat, material removal occurred through the processes of melting and vaporization. Consequently, the pulse-on time emerged as a critical parameter influencing not only the depth of material removal but also the surface quality and the amount of energy delivered to the work piece. In EDM, the primary role of the current was to initiate electrical discharges or sparks between the electrode and the work piece. This phenomenon occurred when a voltage potential was applied across the two components in the presence of a dielectric fluid. The electrical discharges generated during this process produced significant heat at the contact point between the electrode and the work piece. Notably, the current level had a direct impact on the wear of the electrode, with higher currents leading to more substantial wear, thereby reducing tool life and necessitating frequent replacement or treatment of the

Figure 4. EDM setup.

Table 3. Experimental setup

S. No	Description	Conditions
1	Electrode material and size	Copper rod with 110 mm length and 10 mm diameter
2	Work piece	Aged AA7075/12wt.%TiC composite
3	Additive for mixing with dielectric medium	Chromium with average particle size of 15 µm
4	Dielectric medium	Kerosene
5	Polarity	Reverse
6	Dielectric side flushing pressure	1 kgf/cm^2

electrode. In the context of EDM, the control of the current level was a crucial factor in achieving the required accuracy and precision. By regulating the current, it became possible to manage the depth and shape of the machined features with precision. The pulse on and pulse-off parameters have the same effect in opposite poles. Hence, pulse-on is selected as one of the parameters with current. The response parameters were chosen as the TWR and SR. The pulse-on and current directly influenced TWR and SR more than any other input parameters. Besides, the chromium concentration also directly influenced the TWR and SR of AA7075/TiC MMCs. So the pulse-

Table 4. L9 with EDM parameters

Experiment No.	Vol.% chromium (g/litre)	Pulse on time (µs)	Current (amps)
1	0	120	5
2	0	240	10
3	0	360	15
4	4	120	10
5	4	240	15
6	4	360	5
7	8	120	15
8	8	240	5
9	8	360	10

on, current, and chromium concentration were selected as input parameters. The TWR and SR were selected as response parameters due to the enhanced hardness of aged AA7075/TiC MMC. The enhanced hardness of aged AA7075-based composites was difficult to machine in EDM, and it consumed large current, extended pulse on. Besides, high pulse-on and large current caused a decrease in the life of the electrode and heavily affected the surface finish of the machining surface, requiring secondary operations to obtain a greater surface finish. Besides, more research was done by taking material removal rate (MRR) and TWR, and no research has been done on the optimization of EDM process by taking TWR and SR together. The chromium concentration was taken as one of the input parameters, which caused more heat dissipation from the machining area and hence enhanced the life of the electrode and improved surface finish. An additive helped to improve cooling, reduce tool wear, enhance the flushing of debris, improve surface finish, stabilize the spark, and prevent corrosion. The EDM setup was displayed in Fig. 4. The experimental setup was displayed in Table 3. The L9 orthogonal array was chosen for optimization, and it was done by using GRA. The EDM input parameters with L9 OA were displayed in Table 4 (Bharat *et al.*, 2022b).

The GRA was utilized for the optimization of EDM process parameters of the best combination of aged AA7075/TiC MMC. The first step in GRA involved data pre-processing, wherein the TWR and SR experimental data underwent standardization to fit within the zero to one range. This standardization was necessary when there were variations in the range and unit of one dataset compared to another. The purpose of data pre-processing was to transform a sequence into one that is comparable to the original. Multiple methods for data pre-processing in GRA were available, and the selection depended on the specific parameters of the data series. If the inherent property of the original sequence was characterized by "lower-the-better," it should be normalized as outlined in the provided equation (Viswanathan *et al.*, 2021b).

$$y_i^*(\mathrm{k}) = \frac{max\, y_i^{(0)}(k) - y_i^{(0)}(k)}{max\, y_i^{(0)}(k) - min\, y_i^{(0)}(k)}$$

Here, i = 1, 2,..., m, and k = 1, 2,..., n represent the original reference sequence and pre-processed data. The notation $y_i^*(\mathrm{k})$ represents the normalized value, $y_i^{(0)}$ denotes the intended sequence, $min\, y_i^{(0)}(k)$ signifies the minimum value in the sequence, and $max\, y_i^{(0)}(k)$ represents the sequence's maximum value. The total number of observations is n, while the number of experiments is m.

The grey relational coefficient (GRC) is a GRA measure used to assess the applicability of two systems or sequences. The GRC is determined by using the following equation.

$$\gamma y_0(\mathrm{k}), y_i^* = \frac{\Delta_{\min} + \zeta \Delta_{max}}{\Delta_{0i}(k) + \zeta \Delta_{max}}$$

Where Δ_{0i} (k) is also known as the deviation sequence and duplicates the difference between x_0(k) and y_i^* (k). In most circumstances, the value is lower and the distinct ability is greater, hence = 0.5 is used.

The grey relational grade (GRG) is typically derived by taking the average value of the GRC. The GRG is used to assess multi-response characteristics and it is determined by using the equation.

$$\mathrm{GRG} = \frac{1}{n}\sum_{i=1}^{n}(\gamma y_0(\mathrm{k}), y_i^*(\mathrm{k}))$$

The higher the GRG, the closer the linked experimental result is to the ideal normalised value.

3. RESULTS AND DISCUSSION

3.1. Vickers micro hardness test

The AA7075/xTiC (x=0, 4, 8, 12, and 16 wt.%) composites, both aged and non-aged, underwent Vickers microhardness testing. Three trials were

Table 5. Results of Vickers micro hardness test

S. No	Specimens	Vickers micro hardness	
		Non aged AA7075/TiC	Aged AA7075/TiC
1	AA7075	94	106
2	AA7075/4wt.%TiC	109	124
3	AA7075/8wt.%TiC	128	139
4	AA7075/12wt.%TiC	146	158
5	AA7075/16wt.%TiC	138	147

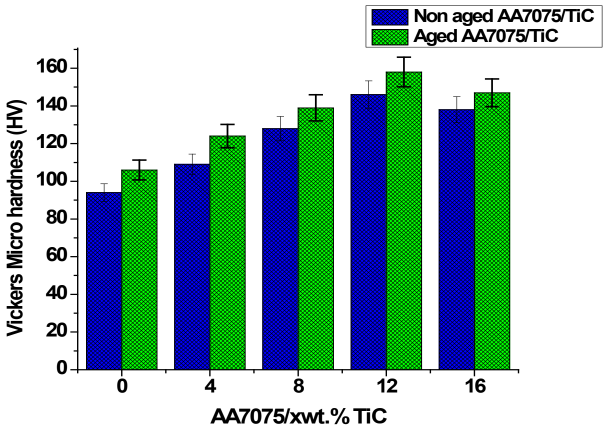

Figure 5. Comparison of results for Vickers hardness test of AA7075/TiC composites.

performed, and the average Vickers microhardness value was utilized to analyze the impact of reinforcement and aging. The results of the Vickers microhardness test are presented in Table 5. Figure 5 illustrates the comparison of Vickers microhardness between aged and non-aged AA7075/TiC MMCs. From the obtained results of microhardness, the aged AA7075/TiC MMCs had higher microhardness than its corresponding non-aged AA7075/TiC MMCs due to the obtained fine grain structure and growth of precipitates. Titanium carbide is a resilient and durable ceramic material. Incorporating TiC reinforces the matrix through solid solution strengthening, a process in which improved hardness results from interactions between alloying elements and the reinforcing particles. Fine particles, including TiC, precipitate and act as efficient hindrances to the movement of dislocations. Dislocations, which are defects in the crystal structure of a material and can contribute to plastic deformation, encounter these obstacles. The presence of these hindrances restricts the mobility of dislocations, making their movement through the material more challenging. This enhanced dislocation pinning contributes to an overall enhancement in microhardness (Alam Mohammad *et al.*, 2023). The enhancement of microhardness in AA7075 resulting from the introduction of titanium carbide (TiC) is primarily attributed to the reinforcing effect of TiC particles within the composite material. As TiC is incorporated into the matrix of AA7075, it acts as a strengthening agent, leading to an augmentation of microhardness. When distributed within the less robust matrix of AA7075, these TiC particles exhibit resistance to deformation, ultimately leading to a general enhancement in the microhardness of the composite.

The presence of TiC particles had the potential to hinder the movement of dislocations within the crystal lattice of the material. Dislocations represented flaws in the crystal structure that could move and play a role in deformation. By restraining dislocation mobility, TiC functioned to fortify the material, leading to a rise in microhardness. Furthermore, the reinforcement from TiC improved the load-bearing capacity of the composite, indicating that these particles effectively carried and distributed applied stresses. This, in turn, reduced the likelihood of localized deformation and contributed to an overall increase in the material's hardness. The addition of titanium carbide into matrix AA7075 improved microhardness value up to 12 wt.% and decreased by 16 wt.% TiC addition in both the aged and non-aged cases. The higher microhardness of 156 HV was obtained at 12 wt.% TiC addition due to the better bonding of TiC with AA7075 and obtained uniform distribution of TiC in matrix AA7075. The concentration of 12 wt.% TiC was probably an optimal equilibrium between reinforcement and the amount of TiC added. This particular concentration provided a sufficient quantity of TiC particles to enhance microhardness without inducing issues such as agglomeration or excessive reinforcing, leading to an overall improvement in hardness. The synergistic effect arising from the optimal bonding and uniform dispersion probably maximized the reinforcing properties of TiC (Fan *et al.*, 2020). In comparison to other concentrations, this synergy contributed to an overall enhancement in microhardness. The correct concentration of TiC diminished the likelihood of structural flaws or disruptions within the matrix. A uniform distribution and strong bonding decreased the presence of voids, discontinuities, or other structural imperfections that could compromise microhardness. The decrease in microhardness with the addition of 16 wt.% of TiC was due to the over-accumulation of TiC into matrix AA7075. The decline in microhardness resulting from incorporating 16 wt.% TiC could stem from factors such as agglomeration, over-reinforcement, interstitial alloying, structural changes, or suboptimal processing conditions (Golla *et al.*, 2023). The specific reasons for this effect would be contingent on the properties of the composite material, the interactions between TiC and the matrix, and the entirety of the manufacturing process.

3.2. Density test

The density of both non-aged and aged AA7075 composites was determined using the Archimedes principle, and the results are presented in Table 6. A comparison of the density of non-aged and aged composites is illustrated in Fig. 6. The incorporation of high-density titanium carbide enhanced the density of AA7075/TiC composites up to a 12 wt.% inclusion and decreased the density with a 16 wt.% inclusion in both aged and non-aged conditions. The addition of TiC, characterized by its high density, contributed to an overall elevation in the composite's density. When these denser TiC particles were uniformly dispersed throughout the matrix, they introduced additional mass to the material, leading to an increased overall density. At concentrations below 12 wt.%, TiC particles had the ability to effectively occupy voids within the matrix, decreasing porosity and fostering a more condensed structure. This filling process resulted in an augmented overall density of the composite (Manohar *et al.*, 2023). Incorporating TiC could lead to heightened porosity and the clustering of particles beyond a certain concentration (16 wt.% in this instance). An excess of TiC might generate spaces or voids between particles, elevating porosity and reducing the material density (Wang *et al.*, 2023). Due to alterations in the composite's microstructure, the density might be influenced by the ageing process. The precipitation and structural changes induced by ageing could affect the distribution and interaction of TiC particles within the matrix, thereby modifying the overall density. The elevated concentration of titanium carbide in the AA7075 matrix increased porosity, leading to a reduction in density. Notably, the highest density was observed in the AA7075/12wt.%TiC composite for both aged and non-aged composites. The higher density of 2.889 g·cm^{-3} was obtained in aged AA7075/12wt.%TiC MMC.

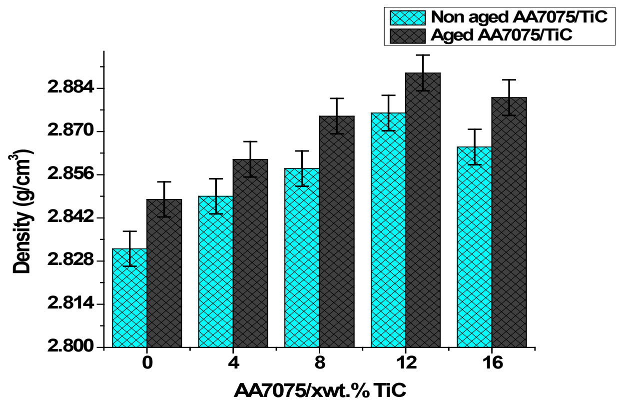

Figure 6. Comparison of results for density test of AA7075/TiC composites.

3.3. Tensile strength

The tensile strength of both non-aged and aged AA7075/TiC MMC was determined by conducting a tensile test. From Fig. 7 and Table 7, it can be concluded that the tensile strength of aged AA7075/TiC MMC was higher than that of its non-aged counterpart. Additionally, the addition of TiC to the AA7075 matrix material enhanced tensile strength up to 12 wt.% but decreased it with the addition of 16 wt.%. The higher tensile strength of 312.8 MPa was obtained from aged AA7075/12wt.%TiC MMC. The introduction of TiC particles into the AA7075 matrix had the potential to enhance the tensile strength through mechanisms such as load transfer, Orowan strengthening, and dislocation pinning (Khan *et al.,* 2022). The aging process resulted in the formation and growth of precipitates, such as the η' (eta prime) phase, contributing to the increased tensile strength of the alloy. The effective reinforcement and strengthening provided by the TiC parti-

Table 6. Results of density test

S. No	Specimens	Density (g·cm^{-3})	
		Non aged AA7075/TiC	Aged AA7075/TiC
1	AA7075	2.832	2.848
2	AA7075/4wt.%TiC	2.849	2.861
3	AA7075/8wt.%TiC	2.858	2.875
4	AA7075/12wt.%TiC	2.876	2.889
5	AA7075/16wt.%TiC	2.865	2.881

Table 7. Results of Tensile strength

S.No	Specimens	Tensile strength (MPa)	
		Non aged AA7075/TiC	Aged AA7075/TiC
1	AA7075	248	258.6
2	AA7075/4wt.%TiC	261.5	269.4
3	AA7075/8wt.%TiC	283.9	292.6
4	AA7075/12wt.%TiC	305	312.8
5	AA7075/16wt.%TiC	296.4	303.4

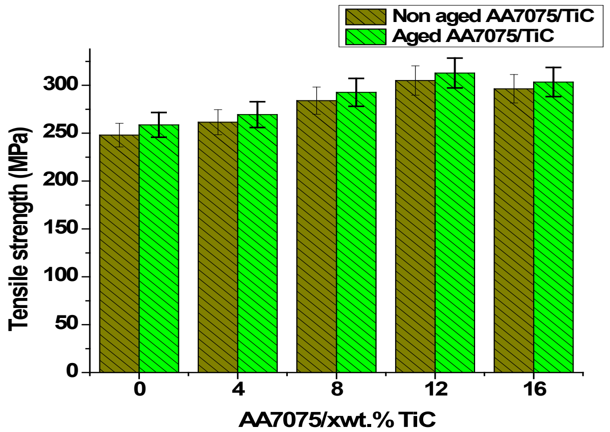

Figure 7. Comparison of results for tensile test of AA7075/TiC composites.

cles could be responsible for the increase in tensile strength of up to 12 wt.% upon the addition of TiC. The bonding strength of TiC with matrix AA7075 is high, which causes the enhancement of tensile strength. Beyond a 16 wt.% concentration, an excess of TiC particles could lead to issues like clustering, agglomeration, or other adverse effects, diminishing the overall effectiveness of reinforcement and potentially inducing stress concentrations. The fractured surfaces of aged AA7075/xTiC (x=0, 4, 8, 12, and 16 wt.%) MMC were analyzed with the help of an SEM. The SEM image of the fractured surfaces of AA7075/TiC MMCs is displayed in Fig. 8. The SEM image of the fractured surface of AA7075 revealed that the fractured surface was due to ductile failure. The addition of TiC into matrix AA7075 converted the fracture mechanism from ductile to brittle. The

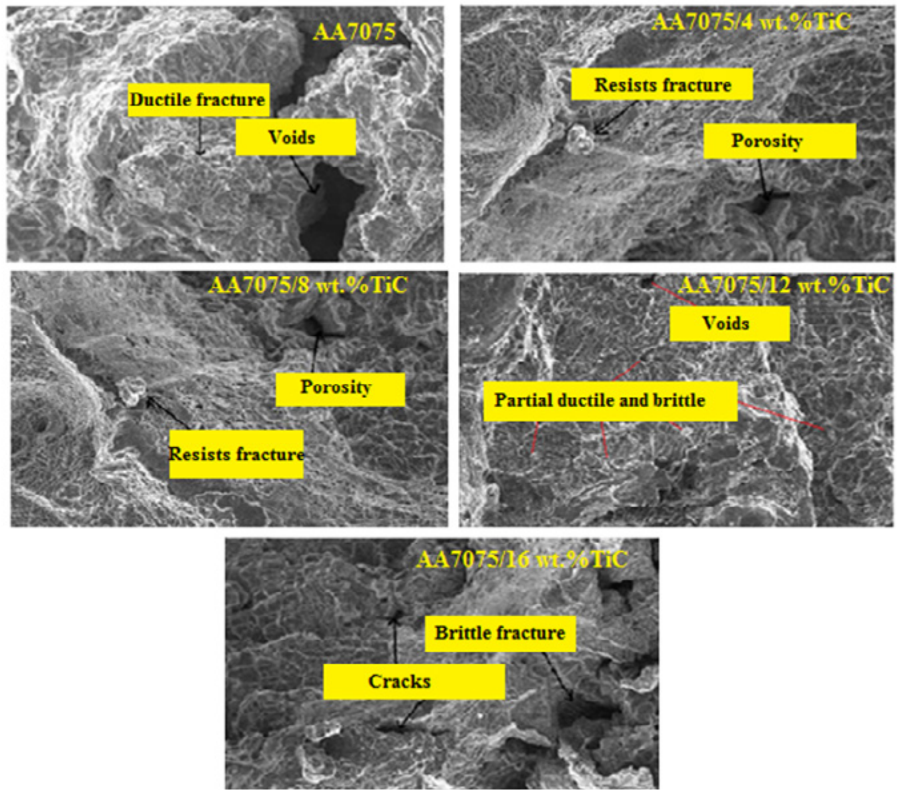

Figure 8. SEM image of fractured surface of tensile tested aged AA7075/TiC composites.

SEM image of AA7075/12wt.%TiC MMC confirmed that the obtained fracture mechanism was partially ductile and partially brittle. The SEM image of the fractured surface of AA7075/16wt.%TIC confirmed that the obtained fracture mechanism was purely brittle. Images from the SEM were useful in analyzing the fracture surface morphology. The presence of a partially ductile and partially brittle fracture in the AA7075/12wt.%TiC MMC implies a more complicated fracture behavior, perhaps involving matrix and reinforcement interactions (Bedolla-Becerril *et al.*, 2023). The purely brittle fracture in the AA7075/16wt.%TiC MMC, on the other hand, indicates that the material is more prone to brittle failure, presumably due to a greater TiC concentration and clustering.

3.4. Compressive strength

The compressive strength of non-aged and aged AA7075/xTiC (x=0, 4, 8, 12, and 16 wt.%) is displayed in Table 8 and Fig. 9. From Fig. 8, the inclusion of TiC into matrix AA7075 improved compressive strength up to 12 wt.% and decreased by 16 wt.% in both non-aged and aged AA7075/TiC MMCs. The higher compressive strength of 326 MPa was obtained from aged AA7075/12wt.%TiC MMC. In the presence of lower TiC concentrations (up to 12 wt.%), the reinforcement had the potential to markedly enhance compressive strength through mechanisms like load-bearing, dislocation prevention, and plastic deformation. The introduction of TiC particles at an optimal concentration could decrease resistance to compression, leading to an overall increase in compressive strength. Upon surpassing the optimal concentration (16 wt.%), the additional TiC particles might initiate adverse effects, including agglomeration or clustering (Sambathkumar *et al.*, 2017). The surplus TiC could induce stress concentrations and act as sites for fracture initiation, leading to a reduction in compressive strength. The clustering of reinforcement might hinder the material's ability to undergo plastic deformation, consequently contributing to earlier failure. Higher concentrations might also lead to uneven distribution or clustering, resulting in localized weaknesses and diminished compressive strength.

3.5. Metallurgical Examination

The aged AA7075/12wt.%TiC composite underwent metallurgical examination such as EDAX and XRD to determine the presence of elements and precipitates. The EDAX microanalysis is displayed in Fig. 10. The elements Al, Ti, C, Zn, Cu, Mg, and Si were present in the aged AA7075/12wt.%TiC MMC.

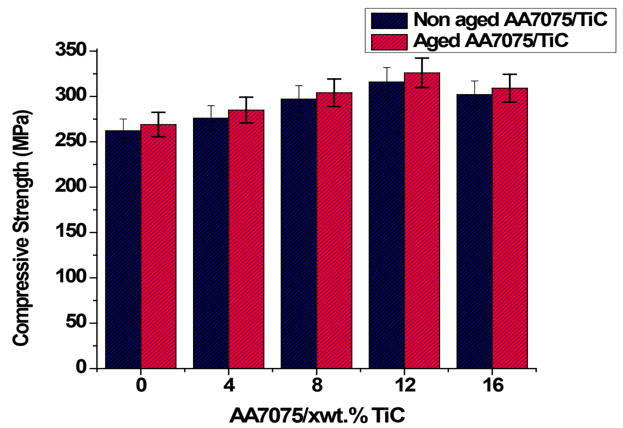

Figure 9. Comparison of results for compression test of AA7075/TiC composites.

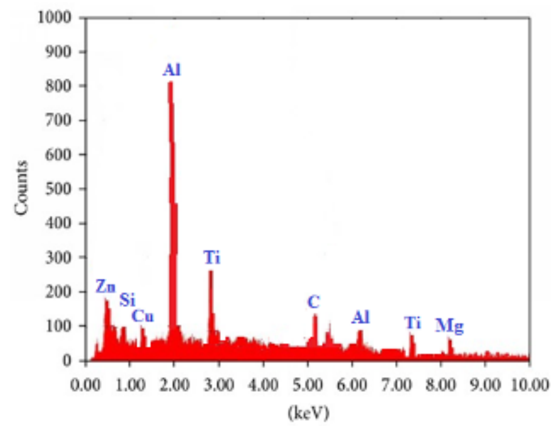

Figure 10. EDAX result of aged AA7075/12wt. %TiC composite.

Table 8. Results of Compressive strength

S. No	Specimens	Compressive strength (MPa)	
		Non aged AA7075/TiC	Aged AA7075/TiC
1	AA7075	262	269
2	AA7075/4wt.%TiC	276	285
3	AA7075/8wt.%TiC	297	304
4	AA7075/12wt.%TiC	316	326
5	AA7075/16wt.%TiC	302	309

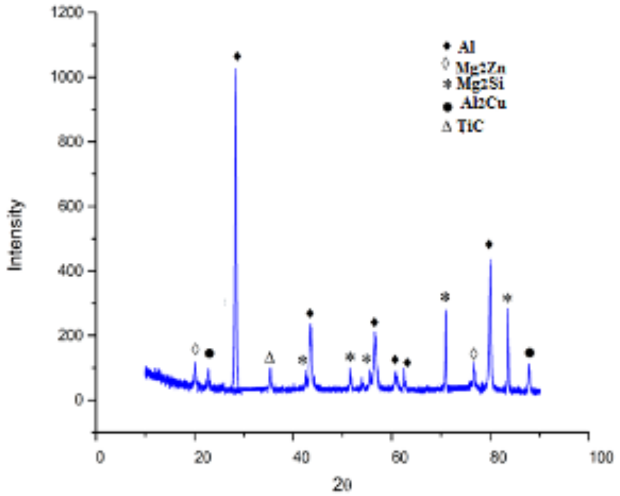

Figure 11. XRD result of aged AA7075/12wt. %TiC composite.

The XRD result of the aged AA7075/12wt.%TiC composite confirmed the presence of precipitation. The XRD pattern is displayed in Fig. 11. The precipitates Mg_2Zn, Mg_2Si, and reinforcement TiC enhanced the micro hardness, density, tensile, and compressive strength (Prakash *et al.*, 2023). The high hardness characteristics of Mg_2Zn, Mg_2Si, and TiC enhanced the mechanical properties of the aged AA7075/12wt.%TiC composite.

The SEM image of the microstructure of the aged AA7075/12wt.%TiC composite is displayed in Fig. 12. The titanium carbide is spread uniformly over the entire matrix material. The SEM image of the aged AA7075/12wt.%TiC MMC reveals that there is no oxide formation. The Mg_2Zn, Mg_2Si, and Al_2Cu precipitates are formed during aging, and they are displayed in the SEM image of AA7075/12wt.%TiC composite. The hard nature of Mg_2Zn and Mg_2Si enhances the micro hardness, tensile, and compressive strength of the aged AA7075/12wt.%TiC MMC. The high ductile property of Al_2Cu enhances the ductile property of the aged AA7075/12wt.%TiC MMC (Rajaram *et al.*, 2022).

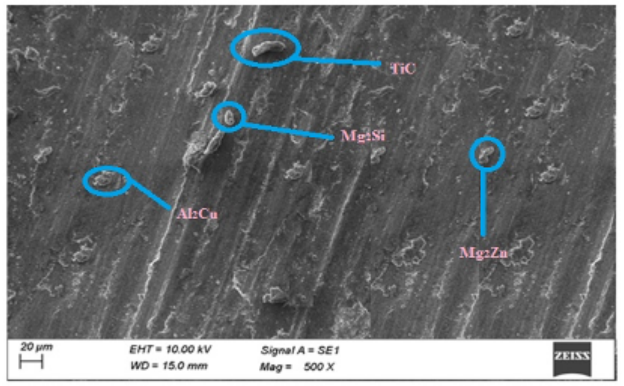

Figure 12. SEM image of aged AA7075/12wt.%TiC composites.

3.6. Optimization of EDM parameters

The optimization of EDM process parameters for the best combination of aged AA7075/12wt.%TiC MMC was performed using GRA optimization. The EDM input parameters for optimization were wt.% of chromium concentration, pulse-on time, and current. The response parameters for optimization were TWR and SR. The L9 orthogonal array was employed for optimization, and Table 9 shows TWR and SR for the L9 input parameters combination. Each combination of EDM input parameters of L9 was set in the EDM machine separately, and responses (TWR and SR) were noted. The TWR and SR for L9 OA were optimized using GRA optimization, which involved normalization, deviation sequence, GRC, and GRG steps. Table 10 displays the results of GRA optimization for EDM process parameters of aged AA7075/12wt.%TiC MMC. A higher value of the normalization value of L8 represents lower TWR and SR, while a lower value of normalization of L3 represents higher TWR and SR. Similarly, higher values of deviation sequence, GRC, and GRG of L8 represent lower TWR and SR, while lower values of these parameters for L3 represent higher TWR and SR. Therefore, the GRA optimization of EDM process parameters for aged AA7075/12wt.%TiC MMC indicates that lower TWR and SR were obtained from the L8 combination of input parameters, while higher TWR and SR were obtained from the L3 combination. The obtained GRG values of TWR and SR were subjected to Taguchi optimization using Minitab 19 software, as shown in Table 11. From the response table, a higher delta value of wt.% of chromium concentration represents the most influencing parameter on GRG, followed by current and pulse-on EDM input parameters. The optimized combination of EDM input parameters is a high level of chromium concentration (8 $g \cdot l^{-1}$), a low level of current (5 amps), and a medium level of pulse-on time (240 µs). The influenced sequence of EDM input parameters is chromium concentration, current, and pulse-on time. The Main effect plot for means of GRG is displayed in Fig. 13, showing that an increase in chromium concentration reduces TWR and SR by improving GRG value, and an increase in pulse-on time reduces TWR and SR up to 240 µs and increases by 360 µs. The increase in current increases TWR and SR due to an increase in heat generation beyond the machining area. The increase in chromium concentration improves heat dissipation capability, resulting in a smooth surface area on the workpiece, and TWR is also reduced. Table 12 provides factor information for ANOVA, displaying the lower, middle, and higher levels of chromium concentration (0, 4, and 8 $g \cdot l^{-1}$), pulse-on (120, 240, and 360 µs), and current (5, 10, and 15 amps). Table 13 presents the ANOVA

Table 9. L9 OA with input and it corresponding response parameters

Experiment No.	Input parameters			Response parameter	
	chromium concentration ($g \cdot l^{-1}$)	Pulse on time (µs)	Current (amps)	TWR ($mg \cdot min^{-1}$)	Ra (µm)
1	0	120	5	0.456	4.78
2	0	240	10	0.603	7.28
3	0	360	15	0.756	9.78
4	4	120	10	0.408	4.28
5	4	240	15	0.555	6.78
6	4	360	5	0.406	4.78
7	8	120	15	0.352	3.78
8	8	240	5	0.208	1.78
9	8	360	10	0.356	4.28

Table 10. GRA optimization

Normalization		Deviation sequence		GRC			RANK
TWR ($mg \cdot min^{-1}$)	Ra (µm)	TWR ($mg \cdot min^{-1}$)	Ra (µm)	TWR ($mg \cdot min^{-1}$)	Ra (µm)	GRG	
0.547	0.625	0.453	0.375	0.525	0.571	0.548	6
0.279	0.313	0.721	0.688	0.410	0.421	0.415	8
0.000	0.000	1.000	1.000	0.333	0.333	0.333	9
0.635	0.688	0.365	0.313	0.578	0.615	0.597	4
0.367	0.375	0.633	0.625	0.441	0.444	0.443	7
0.639	0.625	0.361	0.375	0.581	0.571	0.576	5
0.737	0.750	0.263	0.250	0.656	0.667	0.661	2
1.000	1.000	0.000	0.000	1.000	1.000	1.000	1
0.730	0.688	0.270	0.313	0.649	0.615	0.632	3

Table 11. Response Table for Means

Level	Chromium concentration ($g \cdot l^{-1}$)	Pulse on time (µs)	Current (amps)
1	0.4320	0.6020	0.7080
2	0.5387	0.6193	0.5480
3	0.7643	0.5137	0.4790
Delta	0.3323	0.1057	0.2290
Rank	1	3	2

Table 12. Factor Information

Factor	Type	Levels	Values
Chromium concentration (g/l)	Fixed	3	0, 4, 8
Pulse on time (µs)	Fixed	3	120, 240, 360
Current (amps)	Fixed	3	5, 10, 15

Table 13. Analysis of Variance

Source	DF	Adj SS	Adj MS	F-Value	P-Value	Contribution %
Chromium concentration (g·l^{-1})	2	0.134703	0.067351	6661.13	0.000	64.5
Pulse on time (µs)	2	0.015201	0.007600	751.69	0.041	7.28
Current (amps)	2	0.058608	0.029304	2898.21	0.020	28.1
Error	2	0.002020	0.000010	-	-	0.02
Total	8	0.208532	-	-	-	100

Table 14. Model Summary

S	R-sq	R-sq(adj)	R-sq(pred)
0.0031798	99.99%	99.96%	99.80%

Figure 13. Main effect plot for Means of GRG.

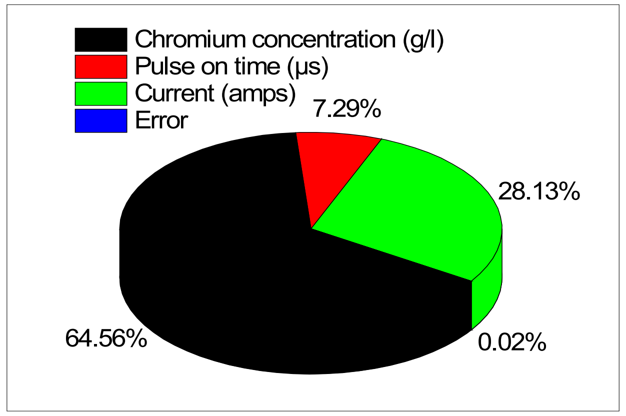

Figure 14. Contribution percentage on GRG.

for GRG of optimized EDM input parameters of aged AA7075/12wt.%TiC MMC. From the ANOVA table, it is confirmed that all input parameters are significant, as the P-value of all input parameters is less than 0.05. The contribution percentage of chromium concentration, pulse-on time, and current input parameters on GRG is 64.5%, 7.28%, and 28.2%, respectively, as depicted in Fig. 14. The figure expresses the contribution of chromium concentration, pulse-on time, and current on GRG. Chromium concentration highly influences GRG, followed by current and pulse-on time. Table 14 displays the model summary for ANOVA of GRG. The obtained adj R square value is 99.96, indicating high reliability of the experimental data and accuracy of the experiment. The confirmation test was conducted for the best combination of 8 g·l^{-1} chromium concentration, 240 µs, and 5 amps current EDM input parameters, and the obtained TWR and SR are 0.198 and 1.56, respectively (Bharat N *et al.*, 2023).

4. CONCLUSIONS

- Stir casting and muffle furnace equipment were used to successfully manufacture aged AA7075/xTiC (x=0, 4, 8, 12, and 16 wt.%) composites. The aged and non-aged AA7075 composites underwent hardness, density tests, tensile, and compression tests following ASTM standards to determine microhardness, density, tensile, and compressive strength. Higher Vickers hardness, density, tensile strength, and compressive strength were obtained from aged AA7075/12wt.%TiC composite. The addition of titanium carbide enhanced hardness and density up to 12 wt.% and diminished by 16 wt.% in both aged and non-aged conditions.
- The mechanical properties of non-aged AA7075/TiC MMC were lower than aged AA7075/TiC MMCs due to the formed precipitates. The higher density of TiC enhanced the density of matrix AA7075. The enhancement of microhardness, tensile strength, and compressive strength resulted from mechanisms like dislocation pinning, load-bearing, dislocation prevention, and plastic deformation. The higher concentration of 16 wt.% TiC decreased hardness, density, tensile strength, and compressive strength due to clustering of reinforcements in the matrix AA7075.
- The higher density of 2.889 g·cm^{-3}, 158 microhardness, 312 MPa tensile strength, and 326 MPa compressive strength were obtained from aged AA7075/12wt.%TiC MMC. The EDS and XRD of aged AA7075/12wt.%TiC confirmed the presence of precipitates, matrix, and reinforcement material. The SEM image of aged AA7075 confirmed that TiC reinforcement was uniformly dispersed in the matrix AA7075 material.
- The better-aged AA7075/12wt.%TiC composite combination underwent optimization of EDM input parameters for TWR and SR. The Taguchi-based GRA was employed for optimization. The influenced EDM input parameters sequence was chromium concentration, current, and pulse-on time. The enhancement of concentration of chromium increased the GRG value and caused a decrease in TWR and SR. The increase in current decreased the GRG value and caused an increase in TWR and SR. The increase in pulse-on time increased GRG value up to 240 µs and decreased by 360 µs. The increase in chromium concentration increased the heat dissipation and flushing of debris, hence decreasing TWR and SR. The optimized combination of EDM input parameters sequence was a high level of chromium concentration (8 g·l^{-1}), low level of current (5 amps), and a medium level of pulse-on time (240 µs). The contribution percentage of chromium concentration, pulse-on time, and current input parameters on GRG was 64.5%, 7.28%, and 28.2%, respectively. The confirmation test was conducted for the best combination of parameters, and the obtained TWR and SR were 0.198 and 1.56, respectively.

REFERENCES

Agrawal, A.P., Srivastava, S.K. (2023). Investigating the Effects of Adding Si3N4 on Microstructural and Mechanical Characteristics of AA7075-based TiB2-Reinforced Hybrid MMCs. I*nt. J. Metal. Cast.* https://doi.org/10.1007/s40962-023-01193-5.

Alagarsamy, S., Ravichandran, M. (2021). Variation of electrode materials and parameters in the EDM of an AA7075-TiO2 composite. *Materials Testing* 63 (2), 182-189. https://doi.org/10.1515/mt-2020-0025.

Alam Mohammad A., Ya, Hamdan B., Azeem, M., Mustapha, M., Yusuf, M., Masood, F., Marode Roshan,V., Sapuan Salit, M., Ansari, Akhter H. (2023). Advancements in aluminum matrix composites reinforced with carbides and graphene: A comprehensive review. *Nanotechnol. Rev.* 12 (1), 0111. https://doi.org/10.1515/ntrev-2023-0111.

Ashok Raj, R., Santhosh, P.A., Prabu, A., Vijayan, S. (2023). Optimization on hardening process parameters of alumnium alloy 7075 based composites using gra approach. *Mater. Res. Express* 10,105007. https://doi.org/10.1088/2053-1591/ad019e.

Balaji, S., Maniarasan, P., Sivakandhan, C., Alagarsamy, S.V. (2023). *Optimization of Machining Parameters in EDM Using GRA Technique*. In: *Advances in Processing of Lightweight Metal Alloys and Composites*. Vignesh, R.V., Padmanaban, R., Govindaraju, M. (eds), Book MHFNN, Springer. https://doi.org/10.1007/978-981-19-7146-4_21.

Bandil, K., Vashisth. H., Kumar, S., Verma, L., Jamwal, A., Kumar, D., Sing, N., Sadassivuni, K., Gupta, P. (2019). Microstructural, mechanical and corrosion behaviour of Al–Si alloy reinforced with SiC metal matrix composite. *J. Compos. Mater.* 53 (28-30), 4215-4223. https://doi.org/10.1177/0021998319856679.

Bedolla-Becerril, E., Garcia-Guerra, J., Lopez-Morelos, V.H., Garcia-Renteria, M.A., Falcon-Franco, L.A., Martinez-Landeros, V.H., García-Villarreal, S., Flores-Villaseñor, S.E. (2023). Tribological Behaviour of Al-2024/TiC Metal Matrix Composites. *Coatings* 13 (1), 77. https://doi.org/10.3390/coatings13010077.

Bharat, N., Bose, P.S.C. (2021). An overview on machinability of hard to cut materials using laser assisted machining. *Mater. Today Proc.* 43 (Part 1), 665-672, https://doi.org/10.1016/j.matpr.2020.12.587.

Bharat, N., Bose, P.S.C. (2022a). Optimization of tribological behaviour of TiO2 nanoparticles reinforced AA7178 alloy matrix using ANN and Taguchi's methodology. *Surf. Topogr.: Metrol. Prop.* 10 (2), 025032. https://doi.org/10.1088/2051-672X/ac7a55.

Bharat, N., Bose, P.S.C. (2022b). A Study on Machining Behaviour of Metal Matrix Composite: A Review. *Advances in Mechanical and Materials Technology. EMSME 2020*, pp. 367-374. Springer, Singapore. https://doi.org/10.1007/978-981-16-2794-1_33.

Bharat, N., Bose, P.S.C., (2023). Wear performance analysis and optimization of process parameters of novel AA7178/nTiO2 using ANN-GRA method. *Proceedings of the Institution of Mechanical Engineers, Part E. Journal of Process Mechanical Engineering* 0(0). https://doi.org/10.1177/09544089231156074.

Burande, S.W., Bhope, D.V. (2021). Review on material selection, tailoring of material properties and ageing of composites with special reference to applicability in automotive suspension. *Mater. Today Proc.* 46 (Part 1), 520-527. https://doi.org/10.1016/j.matpr.2020.10.741.

Chi, Y., Gong, G., Zhao, L., Yu, H., Tian, H., Du, X., Chen, C. (2021). In-situ TiB2-TiC reinforced Fe-Al composite coating on 6061 aluminum alloy by laser surface modification. *J. Mater. Process. Technol.* 294, 117107. https://doi.org/10.1016/j.jmatprotec.2021.117107.

Fan, K., Zhang, F., Shang, C., Saba, F., Yu, J. (2020). Mechanical properties and strengthening mechanisms of titanium matrix nanocomposites reinforced with onion-like carbons. *Compos. Part A Appl. Sci. Manuf.* 132, 105834. https://doi.org/10.1016/j.compositesa.2020.105834.

Foster, A.S.J., Gardner, L., Wang, Y. (2015). Practical strain-hardening material properties for use in deformation-based structural steel design. *Thin-Walled Struct.* 92, 115-129, https://dx.doi.org/10.1016/j.tws.2015.02.002.

Golla, C.B., Babar Pasha, M., Rao, R.N., Ismail, S., Gupta, M. (2023). Influence of TiC Particles on Mechanical and Tribological Characteristics of Advanced Aluminium Matrix Composites Fabricated through Ultrasonic-Assisted Stir Casting. *Crystals* 13 (9), 1360. https://doi.org/10.3390/cryst13091360.

Gupta, V., Singh, B., Mishra, R.K. (2022) Machinability assessment of AA7075 composite reinforced with rice husk ash using spark erosion machining process. *Adv. Mater. Process. Technol.* https://doi.org/10.1080/2374068X.2022.2121075

Gutiérrez, E., Salazar, E., Salinas, A., Deaquino, R., Ponce, A., Yacaman, M., Alducin, D., Ortega, E., Bedolla, A., Fernández, B., Martínez, R., Garay, C. (2023). Texture, microstructure and mechanical properties of AA7075-graphite composites produced through mechanical alloying and hot-extrusion. *Mater. Chem. Phys.* 296, 127323. https://doi.org/10.1016/j.matchemphys.2023.127323.

HassabAlla, M.A.M., Satishkumar, P., Srinivasa Rao, Y., Chebolu, R., Capangpangan, R.Y., Alguno, A.C., Gopal, M., Firos, A., Saravana, M.C. (2022). Investigation of Mechanical Behavior and Microstructure Analysis of AA7075/SiC/B4C-Based Aluminium Hybrid Composites. *Adv. Mater. Sci. Eng.* 2022, ID 2411848 https://doi.org/10.1155/2022/2411848.

Ikubanni, P.P., Oki, M., Adeleke, A.A., Agboola, O.O. (2021). Optimization of the tribological properties of hybrid reinforced aluminium matrix composites using Taguchi and Grey's relational analysis. *Sci. African* 12, e00839. https://doi.org/10.1016/j.sciaf.2021.e00839.

Jebarose, J.S, Udaya Prakash, J., Čep, R., Karthik, K. (2023). Multi-Objective Optimization of Machining Parameters for Drilling LM5/ZrO2 Composites Using Grey Relational Analysis. *Materials* 16 (10), 3615. https://doi.org/10.3390/ma16103615.

Kakaravada, I., Mahamani, A., Pandurangadu, V. (2020). Dry sliding wear behaviour of A356-TiB2/TiC in-situ composites at ambient and elevated temperatures. *Int. J. Mater. Eng. Innov.* 11 (2), 145. https://doi.org/10.1504/IJMATEI.2020.106670.

Khan, A.H., Shah, S.A.A., Umar, F., Noor, U., Gul, R.M., Giasin, K., Aamir, M. (2022). Investigating the Microstructural and Mechanical Properties of Novel Ternary Reinforced AA7075 Hybrid Metal Matrix Composite. *Materials* 15 (15), 5303. https://doi.org/10.3390/ma15155303.

Kumar, H. (2014). Development of mirror like surface characteristics using nano powder mixed electric discharge machining (NPMEDM). *Int. J. Adv. Manuf. Technol.* 76, 105–113. https://doi.org/10.1007/s00170-014-5965-6.

Kumar, A., Kumar, V. (2023). Analysis of Heat Input and its Effects on Microstructure Development and Mechanical Properties of Friction Stir-Processed AA7075 Alloy. *JOM*. https://doi.org/10.1007/s11837-023-06250-2.

Kumar Bhushan, R. (2023). Impact of SiC particle size and weight % on tool life while machining of AA7075/ SiC composite. *J. Alloys Metall. Systems* 3, 100016. https://doi.org/10.1016/j.jalmes.2023.100016.

Manohar, G., Pandey, K.M., Maity, S.R. (2020). Aluminium (AA7075) Metal Matrix Composite Reinforced with B4C Nano Particles and Effect of Individual Alloying Elements in Al Fabricated by Powder Metallurgy Techniques. *J. Phys. Conf. Ser.* 1642, https://doi.org/10.1088/1742-6596/1451/1/012024.

Manojkumar, S., Kant Mehta, K. (2023). Effect of TiB2 on mechanical and corrosion properties of Al 7075/TiB2/Gr composite prepared by stir casting. *Mater. Today Proc.* 91 (Part 1), 62-66. https://doi.org/10.1016/j.matpr.2023.05.033.

Meignanamoorthy, M., Ravichandran, M., Alagarsamy, S.V., Chanakyan, C., Kumar, S.D., Sakthivelu, S. (2020). Effect of various reinforcements on properties of metal matrix composites: A review. *Mater. Today: Proc.* 27 (Part 2), 1118-1121. https://doi.org/10.1016/j.matpr.2020.01.479.

Neuman, E.W., Brown-Shaklee, H., Hilmas, G.E., Fahrenholtz, W.G. (2017). Titanium Diboride-Silicon Carbide-Boron Carbide Ceramics with Super-High Hardness and Strength. *J. Am. Ceram. Soc.* 101 (2), 497-501. https://doi.org/10.1111/jace.15201.

Ogunbiyi, O., Tian, Y., Akinwande, A.A., Lawan Rominiyi, A. (2023). AA7075/HEA composites fabricated by microwave sintering: Assessment of the microstructural features and response surface optimization. *Intermetallics* 155, 107830. https://doi.org/10.1016/j.intermet.2023.107830.

Phaneendra, Y., Mohan Rao, I., Vijaya Kumar, P., Kumari, P.S., Babu, K.S., Ben, B.A., Dhanunjayarao, B.N., Naidu, S.N.V., Hemalatha, S. (2023). Enhancement of tribological properties of AA7075 aluminum alloy using nano-silicon carbide reinforcement: A detailed wear analysis and microhardness study. *Mater. Today Proc. (In Press)* https://doi.org/10.1016/j.matpr.2023.08.135.

Pradhan, S.K., Chatterjee, S., Mallick, A.B., Das, D. (2016). A simple stir casting technique for the preparation of *in-situ* Fe-aluminides reinforced Al-matrix composites. *Perspect. Sci.* 8, 529-532. https://doi.org/10.1016/j.pisc.2016.06.011.

Prakash, J.U., Jebarose Juliyana, S., Salunkhe, S., Gawade, S.R., Nasr, E.S.A., Kamrani, A.K. (2023). Mechanical Characterization and Microstructural Analysis of Stir-Cast Aluminum Matrix Composites (LM5/ZrO2). *Crystals* 13 (8), 1220. https://doi.org/10.3390/cryst13081220.

Prasanna, P., Tallapragada, V.S.S.P.S., Manikanta, B., Aluri, P. (2017). Optimizing The Process Parameters of Electrical Discharge Machining On AA7075 - SiC Alloys. *Mater. Today Proc.* 4 (8), 8517-8527, https://doi.org/10.1016/j.matpr.2017.07.198.

Prianka, B.Z., Saha, S., Rajan Dhar, N. (2020). Hybrid Taguchi-GRA-PCA approach for multi-response optimisation of turning process parameters under HPC condition. *IJMMM* 22 (3-4). https://doi.org/10.1504/IJMMM.2020.107059.

Pulkit, G., Jamwal, A., Kumar, D., Kumar Sadasivuni, K., Hussain, C.M., Gupta, P. (2019). Advance research progresses in aluminium matrix composites: manufacturing & applications. *J. Mater. Res. Technol.* 8 (5), 4924-4939. https://doi.org/10.1016/j.jmrt.2019.06.028.

Rajaram, S., Subbiah, T., Mahali, P.K., Thangaraj, M. (2022). Effect of Age-Hardening Temperature on Mechanical and Wear Behavior of Furnace-Cooled Al7075-Tungsten Carbide Composite. *Materials* 15 (15), 5344. https://doi.org/10.3390/ma15155344.

Rao, V.R., Kumar Mandava, R., Mandava, S., Praveen Kumar, K. (2023). Microstructure, mechanical & wear properties of Aluminium7075-Al2O3-SiC composites. *Mater. Today Proc.* (In Press). https://doi.org/10.1016/j.matpr.2023.08.092.

Rometsch, P.A., Zhang, Y., Knight, S. (2014). Heat treatment of 7xxx series aluminium alloys—Some recent developments. *Trans. Nonferrous Met. Soc. China* 24 (7), 2003-2017. https://doi.org/10.1016/S1003-6326(14)63306-9.

Rui, F., Duan, S., Ma, Y., Luo, J., Liu, C., Lei, H., Chen, H. (2023). Dynamic mechanical properties of nanoparticle-enhanced aluminum alloys fabricated by arc-directed energy deposition. *J. Alloys Compd.* 952, 169997. https://doi.org/10.1016/j.jallcom.2023.169997.

Sairam Varma, G., Reddy, K.S., Reddy, S., Sai, K.V., Kumar, S.M. (2018). The Effect of TiC on Microstructure and Mechanical Properties of AA 2024 MMCs. *IOP Conf. Ser.: Mater. Sci. Eng.* 376, 012085. https://doi.org/10.1088/1757-899X/376/1/012085.

Sakthivelu, S., Sethusundaram, P.P., Meignanamoorthy, M., Dinesh Kumar, S., Chanakyan, C., Alagarsamy, S.V. (2020). Prediction of optimum electric discharge machining parameters for AA7075-SiC composites. *Mater. Today Proc.* 27 (Part 2), 1192-1196, https://doi.org/10.1016/j.matpr.2020.02.082.

Sambathkumar, M., Navaneethakrishnan, P., Ponappa, K., Sasikumar, K.S.K. (2017). Mechanical and Corrosion Behavior of Al7075 (Hybrid) Metal Matrix Composites by Two Step Stir Casting Process. *Lat. Am. J. Solids Struct.* 14 (2), 243-255. https://doi.org/10.1590/1679-78253132.

Sharma, A.K., Bhandari, R., Aherwar, A., Pinca-Bretotean, C. (2020). A study of fabrication methods of aluminum based composites focused on stir casting process. *Mater. Today Proc.* 27 (Part 2), 1608-1612. https://doi.org/10.1016/j.matpr.2020.03.316.

Sharma, J., Nayak, C., Chauhan, P.S., Kumar, R. (2023). Studies and scientific research analysis of aluminium (Al7075) metal matrix composite surface morphology. *Mater. Today Proc.* https://api.semanticscholar.org/CorpusID:261776973.

Selvakumar., S.J., Muralidharan, S.M., Raj, S.D. (2023). Performance analysis of drills with structured surfaces when drilling CFRP/AA7075 stack under MQL condition. *J. Manuf. Process.* 89, 194-219, https://doi.org/10.1016/j.jmapro.2023.01.053.

Sethi, D., Kumar, S., Choudhury, S., Shekhar, S., Saha Roy, B. (2020). Synthesis and characterization of AA7075/TiB2 aluminum matrix composite formed through stir casting method. *Mater. Today Proc.* 26 (Part 2), 1908-1913, https://doi.org/10.1016/j.matpr.2020.02.418.

Seyit, A.K., Özarpa, C., Esen, I., Ahlatci, H., Turen, Y. (2023). Investigation of corrosion behavior of boron carbide reinforced AA7075 powder composites. *J. Alloys Compd.* 968, 172198. https://doi.org/10.1016/j.jallcom.2023.172198.

Sivasamy, A., Ravichandran, M, (2021). Variation of electrode materials and parameters in the EDM of an AA7075-TiO2 composite. *Materials Testing* 63 (2), 182-189. https://doi.org/10.1515/mt-2020-0025.

Tai, C.-L., Tai, P.-J., Hsiao, T.-J., Chiu, P.-H., Tseng, C.-Y., Tsao, T.-C., Chung, T.-F., Yang, Y.-L., Chen, C.-Y., Wang, S.-H., Yang, J.R. (2022). Effect of Natural Ageing on Subsequent Artificial Ageing of AA7075 Aluminum Alloy. *Metals* 12 (10), 1766. https://doi.org/10.3390/met12101766.

Verma, R.K., Parganiha, D., Chopkar, M. (2021). A review on fabrication and characteristics of functionally graded aluminum matrix composites fabricated by centrifugal casting method. *SN Appl. Sci.* 3, 227. https://doi.org/10.1007/s42452-021-04200-8.

Vikas, P., Sudhakar, I., Dilkush, MohanaRao, G., Srinivas, B. (2021). Aging behaviour of hot deformed AA7075 aluminium alloy. *Mater. Today Proc.* 41 (5), 1013-1017, https://doi.org/10.1016/j.matpr.2020.06.117.

Viswanatha, B.M., Prasanna Kumar, M., Basavarajappa, S., Kiran, T.S., Kanchiraya, S. (2021a). Effect of heat treatment and ageing on microstructure for hypoeutectic Al-7Si alloy and hybrid metal matrix composites. *Int. J. Eng. Sci. Technol.* 13 (4), 1-11. https://doi.org/10.4314/ijest.v13i4.1.

Viswanathan, R., Saravanan, K.G., Balaji, J., Prabu, R., Balasubramani, K. (2021b). Optimization of wear and friction parameters in Aluminum7075 hybrid composite. *Mater. Today Proc.* 47 (Part 14), 4449-4453. https://doi.org/10.1016/j.matpr.2021.05.308.

Wang, Y., Monetta, T. (2023). Systematic study of preparation technology, microstructure characteristics and mechanical behaviors for SiC particle-reinforced metal matrix composites *J. Mater. Res. Technol.* 25, 7470-7497, https://doi.org/10.1016/j.jmrt.2023.07.145.

Zhou, B., Liu, B., Zhang, S. (2021). The Advancement of 7XXX Series Aluminum Alloys for Aircraft Structures: A Review. *Metals* 11 (5), 718. https://doi.org/10.3390/met11050718.

Revista de Metalurgia 59(3), July-September 2023, e245, ISSN-L: 0034-8570. https://doi.org/10.3989/revmetalm.245